13th International Conference on
Structural Health Monitoring of Intelligent Infrastructure
DOI: 10.3217/978-3-99161-057-1-188

Experimental assessment of GNSS-smartphone performance in monitoring dynamic motion

Panos Psimoulis[1], Chenyu Xue[1], Jayamanne Oshadee Jayamanne[1], Guangcai Li[2, 3], Jianghui Geng[2, 3]
[1] Nottingham Geospatial Institute, University of Nottingham, United Kingdom

[2] Pride Lab, Wuhan University, Wuhan, China

[3]State Key Lab of Precision Geodesy, The Innovation Academy for Precision Measurement Science and Technology of the Chinese Academy of Sciences
email: panagiotis.psimoulis@nottingham.ac.uk, chenyu.xue@nottingham.ac.uk

ABSTRACT: The recent advancements of GNSS technology have enabled multi-frequency and multi-GNSS observations even at high-rate measurements (up to 100Hz) with a few-mm to cm-level accuracy, broadening the potentials of GNSS application in monitoring dynamic motion of structures. Furthermore, recent studies have revealed the potential of low-cost consumer-grade GNSS receivers in deformation monitoring of civil engineering structures of even cm-level and indicated that the type of GNSS antenna is the main parameter affecting the quality of the GNSS data. In this study, we investigate the potential of dual-frequency smartphone-based GNSS measurements in monitoring dynamic motion of structures. The study is based on controlled experiments of static, slow and dynamic motion of various amplitude and motion frequency, where 1-Hz dual frequency GNSS smartphone measurements are assessed against more accurate geodetic measurements (GNSS and/or Robotic Total Station). The preliminary results show that the GNSS smartphone measurements may suffer from several cycle slips and strong multipath effects, due to the linear polarized GNSS antenna of the smartphone, but in several cases the GNSS smartphone measurements were able to express the dynamic motion. Also, in this study we examine the performance of the GNSS smartphone measurements in monitoring the dynamic response of Wilford Suspension bridge, under various patterns of dynamic loading.
.

KEY WORDS: GNSS-smartphone, deformation monitoring, dynamic motion, shake-table.

1 INTRODUCTION

Smartphones have been adopted in the last decades in many engineering applications. The broad use of smartphones in positioning and navigation applications has benefited from the development of dual-frequency GNSS receivers in some of the advanced smartphone models, enabling those smartphones of dual frequency carrier phase measurements. The first smartphone was Xiaomi Mi 8 (released in 2018) which supports dual frequency GPS/Galileo, single frequency BDS/GLONASS code pseudo-range and carrier phase measurements (Robustelli et al., 2019, Geng and Li, 2019). Nowadays, with the development of more advanced mobile phone chipsets, several smartphone manufacturers are releasing flagship phones supporting features such as L1/E1, L5/E5a dual frequency, multi-GNSS carrier phase measurements capability, etc. Thanks to GPSTest mobile app developed by Barbeau (2023), the capability of recent smartphones as of GNSS performance are crowdsourced and documented in GPSTest database (Barbeau, 2021).

Several studies were conducted focusing on the GNSS-performance of the first dual-frequency GNSS carrier phase Mi8. More specifically, Robustelli et al. (2019) used Xiaomi Mi8 in both single point positioning (SPP) and post-processing kinematic (PPK) applications, showing a RMS accuracy of around 5 m and 1-2 m for the SPP and PPK, respectively. On the other hand, Chen et al. (2019) employed Xiaomi Mi8 for real time precise point positioning and found that the RMS positioning error is 0.81 m and 1.65 m for horizontal and vertical respectively.

Since then, several other studies have been conducted assessing the performance of dual-frequency GNSS-smartphones. Paziewski et al. (2021) assessed the GNSS observation quality of several smartphones, concluding that the smartphone GNSS data are noisier than the geodetic GNSS data, but still feasible to obtain a cm-level static solution. Li and Geng (2019) analysed GNSS measurement error characteristics from Nexus 9 tablets using both embedded and external antennas, revealing that the root mean squared (RMS) accuracy for the SPP is about 10-20 m, and cm-level precision can be achieved for static PPK solutions.

Hence, the first experiments reveal promising results about the quality of the smartphone-based GNSS measurements, indicating that they can achieve cm-level for relative PPK positioning (Pesyna et al., 2014; Wanninger and Heßelbarth, 2020; Geng and Li, 2019; Dabove and Pietra, 2019). However, most of the experiments are based on static experiments and only one study is based on experiments of dynamic motion of smartphone experiments (Vazquez-Ontiveros, et al., 2024).

With the broader trend of applying low-cost GNSS receivers for monitoring applications (Xue et al., 2021; Xue et al., 2022; Xue and Psimoulis, 2023), there is great potential for mobile phones to be used for precise positioning services such as in SHM due to: 1) the relative low-cost with respect the geodetic GNSS receiver, 2) the raw smartphone GNSS measurements (code and carrier phase, etc.) which are accessible to the broader smartphone users community, 3) the potential of crowdsourcing data through the smartphones application, and 4) the availability of various sensors such as accelerometers, gyros, which can be combined with GNSS measurements in SHM applications (Lăpădat et al., 2021).

In general, it is expected that the code and carrier phase measurements of smartphones are of relatively lower quality

DOI: 10.3217/978-3-99161-057-1-188

than those of geodetic receiver. However, it was shown that ambiguity resolution of L1 measurements, which is the prerequisite for achieving a precise solution of cm-levelm, can be achieved, as it was concluded from experimental study using a Huawei P30 smartphone (Wanninger and Heßelbarth, 2020).

Although there are a few studies regarding deformation monitoring with smartphones, most of them, only take advantage of its embedded accelerometer, their GNSS observation functionality is rarely assessed for its deformation monitoring applicability except for few conducted by Zeng et al., (2022) and Vazquez-Ontiveros et al. (2023). Vazquez-Ontiveros et al. (2023) found that an RMS error of 1.4 cm in the horizontal component could be achieved for kinematic circular trajectory with a rotating speed of 0.44 rad/s (~0.07 Hz) and an rotation radius (amplitude) of 19 cm and RMS errors of 0.7 cm, 1.2 cm, and 4.2 cm in the East, North, and Up components could be obtained with static experiment.

In this study, we present the preliminary results of controlled experiments, where smartphone GNSS measurements were conducted to monitor dynamic vertical and horizontal motion and evaluate the performance of the GNSS measurements. The preliminary results are promising, indicating the potential of smartphone GNSS measurements for dynamic motion monitoring.

2 METHODOLOGY

The study was based on two controlled experiments, aiming to simulate long-period/low-frequency (up to 0.2 Hz) cm-level or larger motion, meeting the main deflection characteristics (amplitude and frequency) of flexible structures (e.g., long bridges and tall buildings) under normal service conditions (Meng et al., 2018).

The first experiment involved a controlled vertical periodic motion (of up to 0.1 Hz) produced manually by a platform, following the methodology of the study (Peppa et al. 2018), and monitored by smartphone GNSS receiver and a robotic total station (RTS) measurement. The mm-level accuracy of RTS measurements served as the reference for evaluating the performance of the smartphone GNSS (Psimoulis et al., 2008).

The second experiment focused on controlled horizontal oscillations of up to 0.2 Hz, induced by a shake table. Multiple GNSS sensors, such as survey-grade, low-cost and smartphone-grade receivers, were attached to the shake table, along with several accelerometers, all subjected to the same excitations. The direct trajectory output of the shake table was used as a reference to assess the performance of different sensors. The analysis of the GNSS timeseries, using statistical and spectral techniques, was applied in both experiments to quantify measurement accuracy and identify their dominant frequencies.

3 CONTROLLED VERTICAL EXPERIMENT

The first experimental assessment aimed to evaluate the performance of GNSS-smartphone for monitoring low frequency cm-level vertical dynamic motion. We conducted an experiment on the open roof of Nottingham Geospatial Building (NGB), where periodic vertical oscillations were executed by using a heavy-duty tripod with a height-adjustable platform and manually controlled vertical movement. On the top of the tripod, a 360º-prism and metallic plate were mounted, where the smartphone was securely placed. We manually introduced vertical periodic oscillations of about 0.05 Hz and 0.1 Hz by synchronising to a metronome, as described in Peppa et al., 2018, and the amplitude of 2 to 3 cm was controlled based on the graduation etched on the pole.

The setup of the vertical controlled experiment is shown in Figure 1, where the GNSS base station is consisted of Leica AS10 geodetic antenna and Leica GS10 geodetic receiver, recording in 1 Hz multi-GNSS observations (i.e. GPS, GLONASS, Galileo, BDS; Figure 1A). The Samsung S23 FE, equipped with the dual-frequency GNSS receiver, was set on top of a ground plate, to limit the multipath effect, recording 1Hz multi-GNSS observations, using the GnssLogger App, developed by Google (Google, 2024). The Samsung S23 FE could record L1/L5 GPS, B1i/B2a BDS, E1/E5a Galileo, and G1 GLONASS signals. Finally, the 360º-prism Leica prism was monitored by Leica TS30 RTS, which was recording at 10 Hz sampling-rate (Peppa et al., 2018, Peppa and Psimoulis, 2023).

We conducted six oscillations; (i) three oscillations of approximately 0.1 Hz frequency, and amplitude of ~2 cm (A), and ~3cm (B) and C); and (ii) three oscillations of approximately 0.05 Hz frequency and amplitude of ~1 cm (D),~2 cm (E) and ~3 cm (F).

The RTS ortho-height timeseries relative to the initial position (prior to the oscillation) were exported, expressing the vertical displacement of the oscillation. The smartphone GNSS data were logged in Receiver Independent Exchange Format (RINEX) 3.03 from the GnssLogger App. The GNSS data were post-processed using double-difference (DD) in kinematic mode in RTKLIB demo5 b34h (Everett, 2023) with mobile GNSS data as the rover and Leica GS10 data as the base. The multi-GNSS solutions were obtained using GPS, Galileo and BDS observations. The GLONASS observations were not used for the GNSS solution due to the GLONASS inter-frequency bias between the GNSS smartphone and the GNSS base station, which affects the ambiguity resolution of the GNSS measurements (Msaewe et al., 2017). The Up-component time-series of the GNSS solution reflected vertical oscillation and was compared against the RTS vertical timeseries to evaluate the accuracy of the GNSS smartphone data.

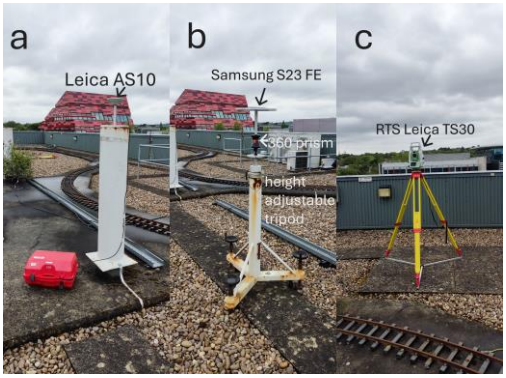

Figure 1. (left) The GNSS base station, (middle) the rover station with the prism and a metallic plate where the Samsung S23 FE has been mounted, and (left) the RTS recording the position of the prism.

DOI: 10.3217/978-3-99161-057-1-188

Figure 2 shows the vertical component timeseries and Discrete Fourier Transform (DFT) spectra of the RTS and GNSS data for the oscillation case of ~0.05 Hz frequency and ~3cm amplitude (case F) respectively. It is clearly observed the pattern of sinusoidal movement in the GNSS timeseries, with a slight downward drift with respect to the RTS timeseries, which can be the result of low-frequency noise due to multipath effect, to which is susceptible the linearly polarised smartphone antenna.

Likewise, Figure 3 are presented the Up-component time-series and the respective spectra of GNSS and RTS data for case C (amplitude of ~3cm, frequency of ~0.1 Hz). As in the experiments of 0.05Hz, it is clearly observed the periodic pattern of the motion followed by both GNSS and RTS data, with the GNSS data characterized also by a low-frequency drift, most likely to multipath effect of the GNSS smartphone measurements.

To quantify the precision of the smartphone GNSS measurement in monitoring the oscillation amplitude, with respect to the RTS timeseries, we estimated the amplitude of the oscillations by using the peak values of each periodic cycle of GNSS and RTS timeseries and calculating the mean oscillation amplitude of each (GNSS and RTS) timeseries. Even though the low-frequency noise of the GNSS timeseries could lead to a drift of about 5-8mm, the estimated oscillation amplitudes of GNSS smartphone data differ from that of the RTS timeseries by 3 cm and 5 cm for the cases F and C, respectively.

Table 1 shows mean amplitude of each experimental vertical motion as it was estimated from the RTS timeseries, the Root Mean Square (RMS) Error of the GNSS timeseries with respect to the amplitude of the RTS and the dominant frequency detected for each oscillation scenario derived from the spectral analysis of the RTS and the smartphone GNSS time-series. It is observed that the GNSS-smartphone precision in detecting the amplitude of the vertical oscillation ranges 2-5 mm. It should be noted though the impact of the low-frequency drift, which may not affect the estimation of the oscillation amplitude but it would affect the estimation of low-frequency semi-static displacement. As for the dominant frequency derivation, the maximum discrepancy between smartphone GNSS and RTS is around 0.007 Hz for 0.1 Hz detection, and 0.003Hz for 0.05Hz detection, equivalent to 6-7% bias in dominant frequency determination. It is also interesting to note that the spectra for RTS timeseries doesn't seem to have distinct peaks but rather shows an area of occurrence of multiple peaks as compared to the smartphone GNSS, indicating that it is more sensitive in differentiating different frequencies in the signal.

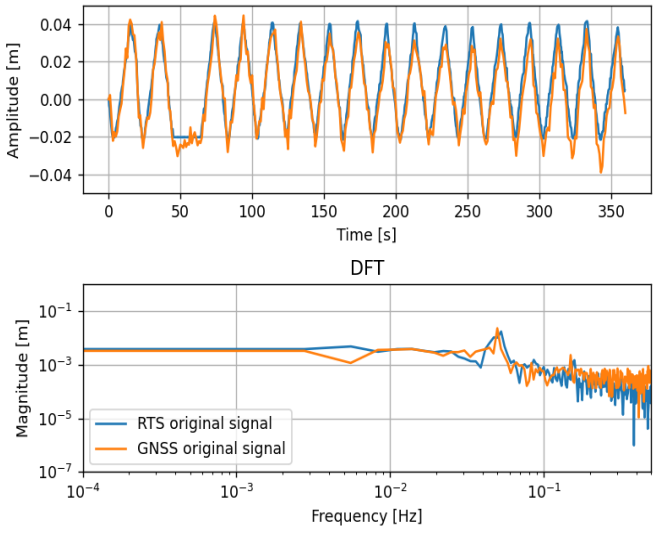

Figure 2. (top) RTS and GNSS-smartphone timeseries for case F oscillation case, and (bottom) the respective spectra

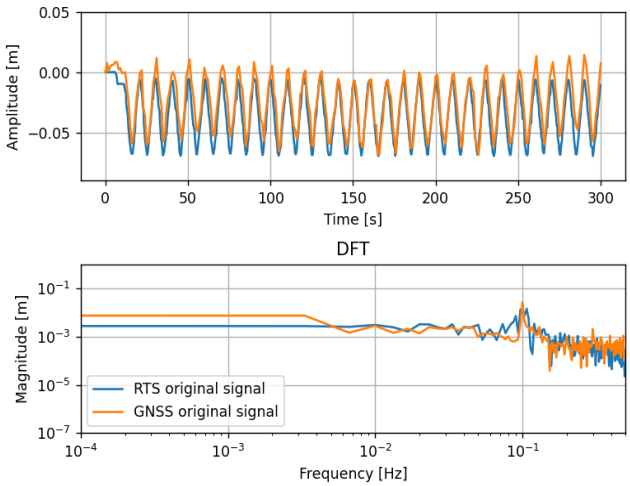

Figure 3. (top) RTS and GNSS-smartphone timeseries for the case C oscillation case, and (bottom) the respective DFT spectra

Table 1. Precision of the smartphone GNSS in monitoring the kinematic oscillatory displacement for scenarios A to F, and the corresponding dominant frequency from RTS and smartphone GNSS for each case

	RTS amplitude (mm)	RMS Error GNSS (mm)	Frequency (Hz)	
			RTS	GNSS
A	21	2.5	0.100	0.100
B	33	2.9	0.100	0.094
C	31	3.2	0.107	0.100
D	11	3.2	0.050	0.050
E	21	2.7	0.050	0.050
F	30	5.1	0.053	0.050

4 CONTROLLED VERTICAL EXPERIMENT

The experiments of horizontal dynamic motion were based on a shake table and it was designed and conducted on the roof of Xinghu Experimental Building at Wuhan University in China. The roof is moderately open with few obstructions by surrounding buildings.

In Figure 5 is presented the experimental setup, where several mobile phones were placed on top of a shake table device, (i) with two smartphones placed outside using their internal GNSS

DOI: 10.3217/978-3-99161-057-1-188

antenna (Huawei P40 and Samsung S23 FE), (ii) two mobile phones placed inside of two shielding boxes (Huawei P40 in the black box and Samsung S23 PE in the white box). The two shielding boxes and the geodetic receiver were both connected to the survey grade antenna via a signal splitter. Inside the two shielding boxes, there were two devices retransmitting the GNSS signal as received by the GNSS geodetic antenna to the smartphone. A patch antenna was also placed on the white shielding box connecting to a u-blox F9P module, and a survey-grade accelerometer was fixed on the side of the shake table.

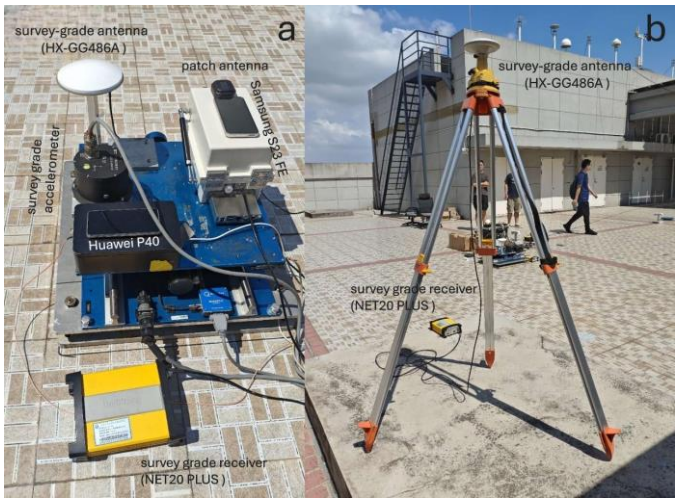

Figure 5. (left) The setup of the rover sensors (GNSS and accelerometer) on the shake table, and (right) the station consisted of survey-grade antenna and receiver

Both the geodetic rover and base station were measuring at a sampling rate of 10 Hz, recording GPS, Galileo, BDS, GLONASS and QZSS observations, while all four smartphones were configured so that the GPS (L1/L5), Galileo (E1/E5a), GLONASS (G1), QZSS (J1/J5), and BDS (B1i/B2a) GNSS raw data were recorded with application GeoDataLogger developed by PrideLab (2024) at a sampling frequency of 1Hz. Additionally, the u-blox receiver recorded GPS, Galileo, GLONASS), QZSS and BDS observations at 10Hz sampling rate.

The accelerometer data were also recorded in GeoDataLogger at the maximum capacity of the smartphone (e.g., around 125 Hz sampling frequency for Samsung and around 100Hz for the rest), while the survey grade accelerometer (TD) recorded at 100 Hz sampling frequency with GPS timestamp thanks to an external GNSS module.

The Quanser Shake Table II, controlled via a MATLAB script implemented in Simulink, was used to perform precise, programmed displacements. The shake table was rigidly bolted to the roof and carefully orientated in E-W direction. We performed in total 25 different motions with various amplitude and oscillating frequency oscillating in E/W direction, with amplitude ranging from 5mm, 10mm, 20mm, 40mm, and oscillation frequency ranging from 0.1 Hz, 0.2Hz, 0.5Hz, 1Hz, 1.5Hz, and 2Hz. Each oscillation lapsed around 2 minutes with at least 1 minute of static period in between consecutive oscillations. The shake table could output direct displacement timeseries at a frequency of 100 Hz, which we employed as the reference data and the ground truth.

It is worth noting that from the experiment,

i) Apart from the GNSS measurements and the geodetic accelerometer data, all other data was not initially synchronised to GNSS time, such as phone accelerometer measurement and shake table output timeseries.
ii) The acceleration timeseries derived directly from the accelerometers output, with the oscillation axis being in East-West direction. The acceleration data of the smartphones were acquired depending on the orientation of each smartphone.
iii) The smartphones can record 1Hz GNSS measurements, meaning that they can be used only for frequencies up to 0.5Hz, due to Nyquist theorem
iv) The ublox measurement terminated halfway during the measurement, causing some data loss.

The GNSS data were post-processed using the open-source software RTKLIB demo5 b34k (Everett, 2024) in the kinematic mode, with the GNSS sensors on the shake table as rover and the geodetic receiver as base forming multiple baselines. The output from the RTKLIB is in E/N/U which is effectively the 3D projection of the baseline vector in the local E/N/U direction. All the GNSS post-processed solutions achieved ambiguity fix.

The synchronisation of the accelerometer and GNSS timeseries is based on finding and shifting the optimum lag when the cross correlation between the geodetic accelerometer and each accelerometer timeseries reached the maximum, indicating strong correlation. By adjusting the time for accelerometer timeseries, we aligned them to GNSS timestamps.

In this study, we focused only on oscillations with frequency motion up to 0.2 Hz, for which the 1 Hz smartphone GNSS data can be used to determine the oscillation frequency, as the Nyquist frequency is 0.5 Hz, based on the sampling rate of the GNSS smartphone data (i.e. 1Hz). The oscillation characteristics (amplitude and oscillation frequency) for the 9 sections from left to right are shown in Table 2. For higher frequencies, the 1-Hz GNSS smartphone data would need to be integrated with accelerometers data. Hence, we investigated only the performance of the 1-Hz GNSS data.

Table 2. Amplitude and frequency of the executed oscillations produced by the shake table.

Oscillation	Amplitude (mm)	Frequency (Hz)
1	5	0.1
2	10	0.1
3	20	0.1
4	40	0.1
5	5	0.2
6	10	0.2
7	20	0.2
8	40	0.2
9	40	0.2

DOI: 10.3217/978-3-99161-057-1-188

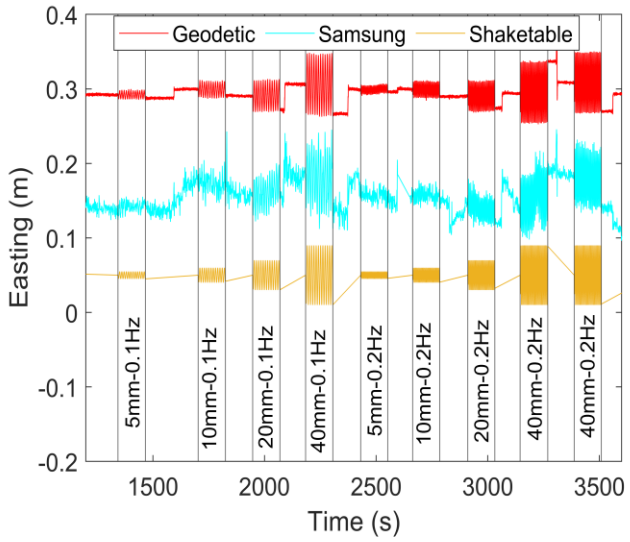

Figure 6. Original timeseries from different GNSS sensors. From top to bottom are 1) geodetic receiver/antenna, 2) Samsung S23 FE 3) output from shake table. The time-series are shifted to avoid overlap between them.

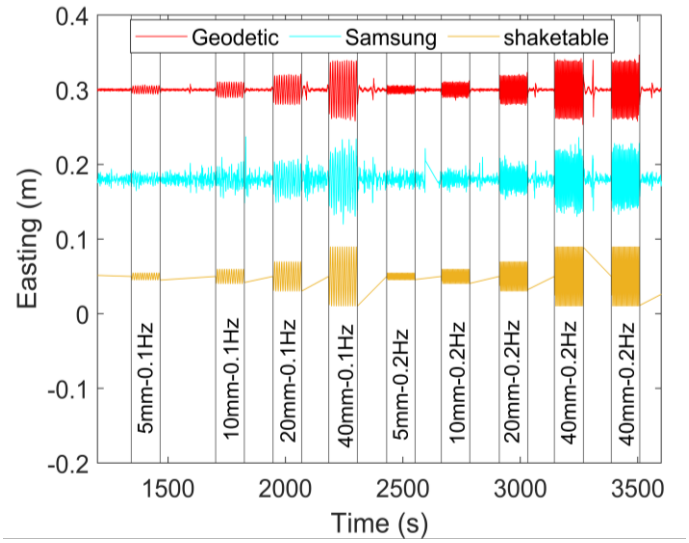

Figure 7. Similar to Figure 6, timeseries from different GNSS sensors but after high-pass filter

The RTKLIB setting for processing GNSS timeseries are utilising L1+L2/E5b+L5/E5a triple frequency option and GPS+Galileo+BDS multi-constellation configuration. Slightly different configuration settings were used for phones using internal antenna and the geodetic antenna due to the significant differences in the antenna since mobile phones antenna is more susceptible to multipath error, cycle slips.

In Figure 6, it is shown the timeseries of the geodetic GNSS receiver and the GNSS smartphone, as they have derived from the GNSS post-process, and the shake table timeseries (i.e. reference data). The start and end time for each oscillation is highlighted by two vertical lines segmenting the timeseries into 9 oscillation sections.

It can be shown in Figure 6 that the geodetic receivers with geodetic antenna time series doesn't seem to be affected by low frequency errors as much as the Samsung timeseries. Also, the noise level is significantly larger for Samsung as compared to geodetic receiver/antenna when the shake table was static. These indicate that the antenna grade is crucial for more precise results less affected by multipath. On the other hand, it is promising that the displacement/excitations could be detected from Samsung timeseries with a strong positive correlation with the geodetic GNSS and shake table timeseries, especially for 20- and 40-mm amplitude oscillations.

To enhance the GNSS timeseries, in terms of reducing the noise level, the GNSS timeseries was firstly filtered using high-pass Chebyshev filter with cutoff frequency of 0.05 Hz to mitigate the multipath bias and potential other source errors. Then, the residuals were calculated by the difference between the GNSS timeseries and the output from shake table.

In Table 3 is shown the true amplitude of each oscillation scenario, as it is derived from the shake table data (i.e. ground truth) and computed RMS error of the geodetic and the smartphone data in estimating the oscillation amplitude. It is observed that the RMSE of the geodetic data does not exceed 2 mm, with the maximum RMS error observed for the scenarios of large oscillation, i.e. 40mm. In all the other scenarios and for amplitude equal or smaller than 20mm, the RMS error is limited to less than 1 mm. Regarding the RMS error of the GNSS smartphone data in estimating the oscillation amplitude the RMS error is generally lower than 5 mm, as it is exceeding the threshold of 5 mm only for two scenarios of oscillations, i.e. 10 and 40mm for 0.1 Hz oscillation frequency. In general, the RMS error of the GNSS smartphone data is about two to four times larger than the geodetic solution. As expected, the overall performance of the GNSS smartphone data is lower, in terms of noise/errors, comparing it to the GNSS geodetic receiver, mainly due to the lower quality of the antenna, since the geodetic receiver/antenna are dedicated GNSS instruments, whereas the mobile phones has comparatively lower grade receiver and antenna. Also, it is observed that the GNSS smartphone has low performance in estimating the oscillation amplitude for the cases of 5 and 10 mm, as the achieved precision is of 3-6.5 mm level, while the results seem more promising for the cases of oscillation amplitude of 20 and 40 mm.

Table 3. Standard deviation of the residuals for different GNSS sensors with reference to Shake table timeseries

Oscillation Scenario	True amplitude (mm)	RMS Error (mm)	
	Shake Table	Geodetic	Smartphone
1 (0.1Hz)	5	0.8	4.0
2 (0.1Hz)	10	0.6	7.6
3 (0.1Hz)	20	0.7	4.3
4 (0.1Hz)	40	1.6	6.9
5 (0.2Hz)	5	0.8	3.6
6 (0.2Hz)	10	0.5	1.9
7 (0.2Hz)	20	0.7	2.3
8 (0.2Hz)	40	1.1	4.0
9 (0.2Hz)	40	1.5	2.5

DOI: 10.3217/978-3-99161-057-1-188

In Figure 8 are presented the spectra of GNSS geodetic and GNSS smartphone timeseries of the experiment of 0.2 Hz and amplitude 20mm, as a representative spectral analysis of all the conducted experiments of oscillations. The spectrum of the GNSS smartphone data is limited to 0.5 Hz, as the sampling-rate was 1 Hz, whereas the GNSS geodetic timeseries is limited to 5 Hz, due to the respective 10 Hz sampling rate. It is clear that the oscillation frequency is accurately detected by both GNSS timeseries. The smartphone GNSS timeseries is characterized by higher noise level, especially for the frequency range higher than 0.2 Hz, as the frequency peaks correspond to higher amplitude, reflecting the more noisy data of GNSS smartphone with respect the GNSS geodetic data. For frequencies lower than 0.05 Hz, the noise has been limited due to the application of the high-pass filter.

In Table 4 are presented the dominant frequencies as they are estimated based on the spectral analysis of the GNSS geodetic data and the GNSS smartphone data and compared based on the frequencies of the oscillation as they derive from the shake table data (i.e. ground truth). It can be observed that frequencies estimated from the smartphone GNSS data deviate not more than 2-3% from the reference frequency derived from shake table output timeseries. Even though, for the oscillations of low amplitude (i.e. 5 and 10mm), the GNSS smartphone suffer from low-frequency noise resulting in ambiguous waveform, the dominant frequency for the oscillation could still be retrieved accurately. Similarly, we conducted DFT for the original timeseries. The frequency that can be detected from the original timeseries is shown in Table 4.

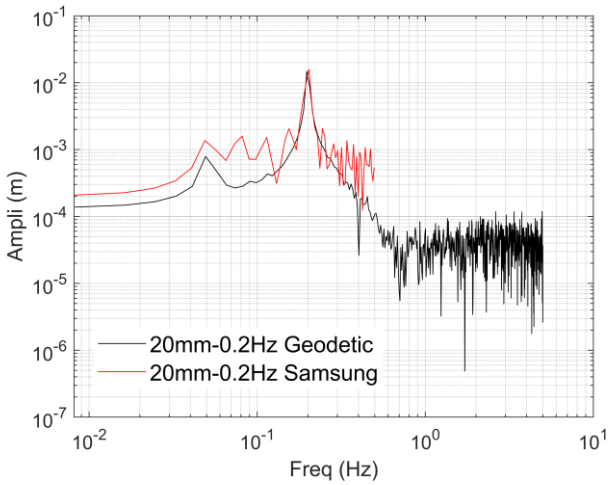

Figure 8. Spectra of GNSS geodetic and GNSS smartphone timeseries of the oscillation of 20mm amplitude ad 0.2 Hz frequency.

Table 4. Dominant frequency derived from each sensor, the percentages in brackets indicate the deviation in percentage from the reference dominant frequency derived from DFT of shake table timeseries.

	Frequency (Hz)		
	Geodetic	Samsung	Shake table
1	0.098 (2%)	0.098 (2%)	0.096
2	0.099 (2%)	0.098 (1%)	0.097
3	0.098 (2%)	0.098 (2%)	0.096
4	0.098 (2%)	0.098 (2%)	0.096
5	0.197 (-2%)	0.197 (-2%)	0.202
6	0.200 (-1%)	0.203 (0%)	0.203
7	0.197 (-3%)	0.203 (0%)	0.203
8	0.197 (-3%)	0.203 (0%)	0.203
9	0.202 (2%)	0.200 (1%)	0.199

5 CASE STUDY: WILFORD BRIDGE MONITORING CAMPAIGN

To evaluate the feasibility of using smartphones for monitoring purposes, a preliminary monitoring campaign was carried out on Wilford Suspension bridge, a test site adopted for many experimental research projects of application of GNSS and surveying techniques in bridge SHM studies (Peppa et al., 2018, Psimoulis et al., 2016). We deployed several different grades of GNSS receivers ad Robotic Total Stations (RTS) on the bridge, to assess the performance of the various GNSS receivers, using the RTS as the ground truth (Psimoulis and Stiros, 2008). For this tudy we focused on the analysis of a geodetic grade GNSS station (GS04) consisted of Leica GS10 receiver ad AS10 antenna, and a smartphone Samsung S23. The GSS receiver were recording simultaneously the response of the bridge under the pedestrians' excitations, with the geodetic GSS receivers recording at 10 Hz sampling rate, while the smartphone was recording at 1 Hz sampling rate.

In Figure 9 are presented the vertical Up) GNSS timeseries of the geodetic and the smartphone, and it is obvious the higher noise level of the smartphone GNSS timeseries, indicating the larger GNSS receiver noise and the significant larger unpressed multipath effect (Peppa and Psimoulis, 2023).

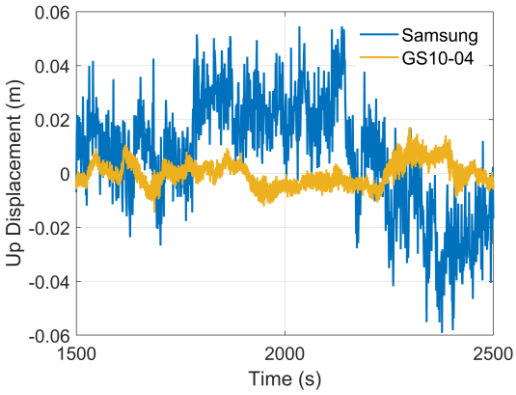

Figure 9. The GNSS timeseries from the geodetic grade GNSS station (GS04) and the smartphone Samsung S23 GNSS receiver. Both GNSS receivers are located at the midspan of the bridge.

To mitigate the low-frequency errors, a high pass filter with cut-off frequency of 0.05 Hz was applied. In Figure 10 are shown the filtered GNSS timeseries of the GS04 geodetic receiver and the smartphone, whereas several activities can be identified from the GS04 timeseries, whilst those response could not easily be identified in the Samsung timeseries,

DOI: 10.3217/978-3-99161-057-1-188

probably due to i) the relatively high bridge modal frequency exceeding the Nyquist frequency of the GNSS smartphone recorded data and ii) the overall high noise level.

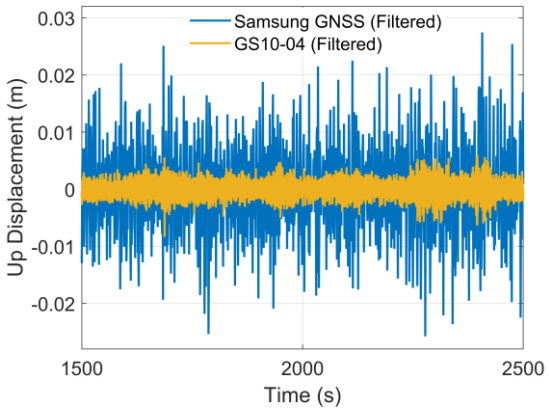

Figure 10. The same plot as Figure 9 presenting the highpass filtered GNSS timeseries of the geodetic and smartphone data.

To unveil the bridge displacements limited by the smartphone GNSS low sampling rate, a common approach is the integration of GNSS with accelerometer data. We adopted loosely coupled data integration using Kalman filter Rauch-Trung-Striebel smoothing algorithm. It could be seen in Figure 11 that the noise from the fused timeseries is greatly reduced from GNSS only solution. A few excitations are also identifiable in correlation with Leica geodetic timeseries and the acceleration timeseries.

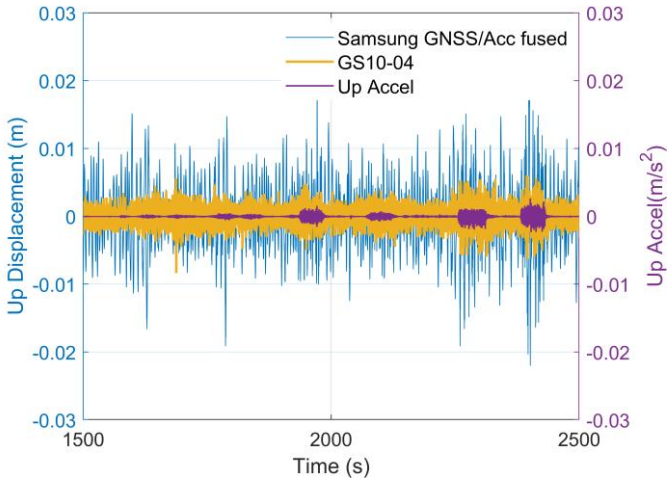

Figure 11 The highpass filtered timeseries of Leica geodetic GS04 solution, the smartphone solution after GNSS and acceleration data integration and the acceleration (after offset removal and scaling) timeseries

6 CONCLUSION

In this study, we analysed the performance of smartphones in monitoring vertical and horizontal oscillations with controlled oscillation setups, particularly for low frequency and low amplitude displacement, with frequency less than 0.5 Hz, and amplitude less than 4 cm.

Based on the controlled experiments of horizontal and vertical motion recorded by smartphones with capacity of GNSS L1/L5, E1/E5a, dual frequency it is observed that it can detect the dynamic oscillation pattern in all cases. The dominant oscillation frequency was accurately detected in all cases meeting the same accuracy as that of geodetic GNSS data. Regarding the estimation of the oscillation amplitude, it is proved to be more noisy than the geodetic GNSS data, at is expected due to the susceptible to multipath effect of the linearly polarized GNSS antenna of the smartphones. The RMS error of estimating the oscillation amplitude ranges between 2 and 5 mm in most cases while the respective one for GNSS geodetic data was not more than 2 mm. More specifically, for oscillation amplitude less than 10mm, the estimation of the oscillation amplitude is more noisy, due to the relative high noise level of smartphone GNSS data, but for the estimation of the frequency it is proved very accurate. For oscillation amplitude larger than 10mm, the results of the GNSS smartphone data seemed to be more promising.

However, due to 1 Hz sampling rate from the mobile phone, the oscillation above 0.5 Hz could not be detected due to aliasing. Therefore, in the future research, we aim to investigate the sensor fusion between high frequency accelerometer measurement and GNSS measurement for detection of higher frequency displacement, which will allow further application of GNSS smartphone data in structural health monitoring (Xue et al., 2024).

ACKNOWLEDGEMENTS

This work is funded by Royal Society International Exchange Collaboration grant with National Natural Science Foundation of China (IEC\NSFC\223184).

REFERENCES

Barbeau, S. (2021). Crowdsourcing GNSS features of Android devices. https://bit.ly/gpstest-device-database

Barbeau, S. (2023). GPSTest. [Mobile app] Google play store. Available at https://play.google.com/store/apps/details?id=com.android.gpstest&hl=en_GB

Chen, B., Gao, C., Liu, Y., & Sun, P. (2019). Real-time precise point positioning with a Xiaomi MI 8 android smartphone. *Sensors*, *19*(12), 2835.

Dabove, P., & Di Pietra, V. (2019). Towards high accuracy GNSS real-time positioning with smartphones. *Advances in Space Research*, *63*(1), 94-102.

Everett, T. (2023). RTKLIB: demo5 b34h. Accessed December 05, 2024. https://github.com/rtklibexplorer/RTKLIB/releases/.

Everett, T. (2024). RTKLIB: demo5 b34k. Accessed December 05, 2024. https://github.com/rtklibexplorer/RTKLIB/releases/.

Geng, J., & Li, G. (2019). On the feasibility of resolving Android GNSS carrier-phase ambiguities. *Journal of Geodesy*, *93*(12), 2621-2635.

Google. (2024). GnssLogger App. [Mobile app] Google play store. Available at https://play.google.com/store/apps/details?id=com.google.android.apps.location.gps.gnsslogger&hl=en_GB

DOI: 10.3217/978-3-99161-057-1-188

Li, G., & Geng, J. (2019). Characteristics of raw multi-GNSS measurement error from Google Android smart devices. *GPS solutions*, *23*(3), 90.

Msaewe, H. A., Hancock, C. M., Psimoulis, P. A., Roberts, G. W., Bonenberg, L., & de Ligt, H. (2017). Investigating multi-GNSS performance in the UK and China based on a zero-baseline measurement approach. *Measurement*, *102*, 186-199.

Paziewski, J., Fortunato, M., Mazzoni, A., & Odolinski, R. (2021). An analysis of multi-GNSS observations tracked by recent Android smartphones and smartphone-only relative positioning results. *Measurement*, *175*, 109162.

Peppa, I., & Psimoulis, P. A. (2023). Detection of GNSS antenna oscillatory motion and multipath conditions via exploitation of multipath-induced SNR variations. *GPS Solutions*, *27*(3), 117.

Peppa, I., Psimoulis, P., & Meng, X. (2018). Using the signal-to-noise ratio of GPS records to detect motion of structures. *Structural control and health monitoring*, *25*(2), e2080.

Pesyna, K. M., Heath, R. W., & Humphreys, T. E. (2014, September). Centimeter positioning with a smartphone-quality GNSS antenna. In *Proceedings of the 27th International Technical Meeting of the Satellite Division of The Institute of Navigation (ION GNSS+ 2014)* (pp. 1568-1577).

Psimoulis, P., Stiros, S. (2008). Ecperimental assessment of the accuracy of GPS and RTS for the determination of the parameters of oscillatin of major structures. *Computer Aided Civil and Infrastructure Engineering*, 23(5), 389-403.

Psimoulis, P., Pytharouli, S. Karambalis, D., Stiros, S. (2008). Potential of Global Positioning System (GPS) to measure frequencies of oscillations of engineering structures. *Journal of Sound and Vibration*, 318(3), 606-623.

Psimoulis, P., Peppa, I., Bonenberg, L.K., Ince, S., Meng, X. (2016). Combination of GPS and RTS measurements for the monitoring of semi-static and dynamic motion of pedestrian bridge, Proc. of 3rd Joint International Symposium on Deformation Monitoring, Vienna, Austria, Austria, 30 March - 1 April 2016. available https://fig.net/resources/proceedings/2016/2016_03_jisdm_pdf/reviewed/JISDM_2016_submission_103.pdf

PrideLab. (2024). Smartphone multi-frequency GNSS and IMU data acquisition. available at https://github.com/PrideLab/PRIDE-GeoDataLogger/tree/main

Robustelli, U., Baiocchi, V., & Pugliano, G. (2019). Assessment of dual frequency GNSS observations from a Xiaomi Mi 8 Android smartphone and positioning performance analysis. Electronics, 8(1), 91.

Vazquez-Ontiveros, J. R., Martinez-Felix, C. A., Melgarejo-Morales, A., Retegui-Schiettekatte, L., Vazquez-Becerra, G. E., & Gaxiola-Camacho, J. R. (2024). Assessing the quality of raw GNSS observations and 3D positioning performance using the Xiaomi Mi 8 dual-frequency smartphone in Northwest Mexico. *Earth Science Informatics*, *17*(1), 21-35.

Wanninger, L., & Heßelbarth, A. (2020). GNSS code and carrier phase observations of a Huawei P30 smartphone: Quality assessment and centimeter-accurate positioning. *GPS Solutions*, *24*(2), 64.

Xue, C., & Psimoulis, P. A. (2023). Monitoring the dynamic response of a pedestrian bridge by using low-cost GNSS receivers. *Engineering Structures*, *284*, 115993.

Xue, C., Psimoulis, P. A., & Meng, X. (2022). Feasibility analysis of the performance of low-cost GNSS receivers in monitoring dynamic motion. *Measurement*, *202*, 111819.

Xue, C., Psimoulis, P., Zhang, Q., & Meng, X. (2021). Analysis of the performance of closely spaced low-cost multi-GNSS receivers. *Applied Geomatics*, *13*(3), 415-435.

Xue, C., Psimoulis, P.A., Hancock, C., Ochieng, F.X., Yang, Y., Li, C., Bhatia, P., Li, Y., Tang, X., (2024), Analysis of the performance of GNSS receiver in monitoring the behaviour of the wind turbine nacelle, Engineering Structures, 317, 118633.